Pharm Res (2015) 32:3886–3898
DOI 10.1007/s11095-015-1748-5

RESEARCH PAPER

PLGA-Based Nanoparticles: a Safe and Suitable Delivery Platform for Osteoarticular Pathologies

Mathieu Riffault[1] • Jean-Luc Six[2] • Patrick Netter[1] • Pierre Gillet[1] • Laurent Grossin[1]

Received: 5 May 2015 / Accepted: 26 June 2015 / Published online: 2 July 2015

ABSTRACT

Purpose Despite the promising applications of PLGA based particles, studies examining the fate and consequences of these particles after intra-articular administration in the joint are scanty. This study was carried out to evaluate the neutrality of the unloaded delivery system on different articular cell types. To facilitate tracking, we have thus developed a fluorescent core of particles, combined to a hyaluronate shell for cell recognition.

Methods Fluorescence pictures were taken at time intervals to assess the internalization and the corresponding inflammatory response was monitored by RT-qPCR and biochemical measurements. After NPs pre-treatment, mesenchymal stem cells (MSCs) were cultured into chondrogenic, adipogenic or osteogenic differentiation media, to investigate if NPs exposure interferes with differentiation ability. Finally, intra-articular injections were performed in healthy rat knees and joint's structure analysed by histological studies.

Results Particles were detected in cytoplasm 8 h after exposure. Internalization led to a slight and reversible increase of inflammatory markers, but lower than in inflammatory conditions. We have confirmed particles exposure minimal neutrality on MSCs pluripotency. Histological exams of joint after intra-articular injections do not demonstrate any side effects of NPs.

Conclusions Our findings suggest that such a delivery platform is well tolerated locally and could be used to deliver active molecules to the joint.

KEY WORDS hyaluronate · nanoparticles · osteoarticular · PLGA · vectorization

ABBREVIATIONS

BSA	Bovine seric albumin
Cy3	Cyanine 3
DAPI	4′,6-diamidino-2-phenylindole
DM	Differentiation medium
FITC	Fluorescein isothiocyanate
HA	Hyaluronic acid
HES	Haematoxylin Eosin Saffron
IA	Intra-articular
LDH	Lactate deshydrogenase
LPS	Lipopolysaccharide
MbT	Mycobacterium tuberculosis
MSCs	Mesenchymal stem cells
MTT	3-(4,5-dimethylthiazol-2-yl)-2,5-diphenyltetrazolium bromide
NO	Nitric oxide
NPs	Nanoparticles
NSAIDs	Non steroidal anti-inflammatory drugs
OA	Osteoarthritis
PBS	Phosphate Buffer Saline
PFA	Paraformaldehyde
PGE_2	Prostaglandins E2
PLGA	Poly (lactic-co-glycolic) acid
rAAV	Recombinant adeno-associated virus

Electronic supplementary material The online version of this article (doi:10.1007/s11095-015-1748-5) contains supplementary material, which is available to authorized users.

✉ Pierre Gillet
pierre.gillet@univ-lorraine.fr

[1] Ingénierie Moléculaire et Physiopathologie Articulaire, Unité Mixte de Recherche 7365, Centre National de la Recherche Scientifique – Université de Lorraine, Biopôle de l'Université de Lorraine, Campus Biologie Santé, 9 Avenue de la Forêt de Haye CS 50184, 54505 Vandœuvre Lès Nancy cedex, France

[2] Laboratoire de Chimie-Physique Macromoléculaire, Unité Mixte de Recherche 7568, Centre National de la Recherche Scientifique – Institut National Polytechnique de Lorraine, ENSIC, Nancy, France

INTRODUCTION

Drug targeting is a major challenge in coming decades in the context of personalized medicine. Current treatments for rheumatic diseases, *e.g.*, NSAIDs, are mostly symptomatic and commonly associated with gastro-intestinal, hepatic, renal and/or cardiac adverse events, especially among the elderly. This makes intra-articular (IA) and cell therapies attractive options notably for patients with localized osteoarthritis (OA) limited to one or several synovial joints. Additionally, IA administration may provide a higher concentration of the medication in the joint macro- and microenvironments, including cartilage and synovium and may avoid systemic effects. To increase and maintain their therapeutic efficacy, drugs can be encapsulated into nanoparticles (NPs), and then delivered to specific sites by passive or active targeting [1]. Furthermore, IA injection of autologous MSCs seems promising in rheumatic disease because they combine both anti-inflammatory and immunosuppressive properties and can initiate cartilage repair by differentiating into chondrocytes [2]. Nanoparticle-based MSCs therapy may therefore be helpful in both cartilage repair and drug delivery.

Among the various carriers proposed for drug delivery, including liposomes, inorganic particles, cyclodextrin, utilization of poly lactic-co-glycolic acid (PLGA) to produce nano or microparticles appears promising [3]. Indeed, PLGA is biocompatible, biodegradable, and belongs to a family of FDA-approved biodegradable polymers. Hydrolysis of PLGA leads to two monomers: lactic acid and glycolic acid. These monomers are endogenous, and can be metabolized by cells *via* Krebs cycle [4]. Given the recent advances in synthesis and surface modification technologies, PLGA can be fine tuned to modify their size, loading (nucleic acid [5], drugs [6], or proteins [7] have been vectorized so far), degradation, and the shell of particles. Due to their biodegradability, PLGA particles are also used to ensure a controlled, sustained release of drugs [8].

Active targeting with functionalization of particles surface enables to direct them to designated targets, through enhancement of cell interaction and internalization. Several recent studies have addressed the question of shell improvement by functionalization (by chemical modification of the shell [9], grafting peptides [10] or antibodies [11]). An interesting approach developed by *Arpicco S et al.* [12] was to target CD44, a cell-surface glycoprotein expressed by many cell types, by covering particles with its major ligand: hyaluronic acid (HA). Since CD44 is overexpressed in tumor cells and plays a key role in metastasis, targeting CD44 with HA-covered particles has demonstrated a great potential to improve drug delivery [13]. CD44 is also expressed in articular cells and involved in matrix attachment and signal transduction [14, 15]. HA is a major component of extracellular matrix and synovial fluid and is internalized by chondrocytes through CD44 binding [16]. HA-covered active particles represent therefore a novel and attractive therapeutic approach in the joint [17].

Patients suffering from distinct articular pathologies such as rheumatoid arthritis (a chronic inflammatory disease) or osteoarthritis (a degenerative rheumatic condition) could benefit from such particular drug/cell delivery system. Despite the recent improvement in rheumatic therapy [18], one of the major issues is still to find an appropriate administration route for active compounds, regardless of the aetiology of the disease. Due to a lack of vasculature of cartilage and the filtering capacity of synovial membrane, a local administration by intra articular injection is conducive to more persistent drug availability than intravenous injection or oral administration. However, clearance of drug from synovial fluid could be inadequate, and repeated intra articular injections are risky because they may lead to severe side effects [19].

In our earlier work, particles with a hyaluronate shell were developed and synthesized by a double emulsion and solvent evaporation method. The size of particles encapsulating fluorescent molecules (dextran coupled FITC) is 450 ± 20 nm [20, 21]. Based on this work, we have modified the production process in order to develop a fluorescent labelling of the NPs' core, by replacing a fraction of Bovine Serum Albumin (BSA) (used for stabilization of the emulsion) by BSA conjugated to cyanine-3 dye. The resulting traceable, HA-covered, unloaded NPs were then used to investigate whether labelled NPs could be used as an appropriate drug delivery system into the joint. Here, the internalization and the safety/toxicity of HA-NPs on human articular cells was investigated *in vitro*, using primary cultures of synoviocytes and chondrocytes. While the relative harmlessness of HA-NPs internalization on human bone MSCs differentiation was evaluated by using *in vitro* culture systems, the safety/tolerability of intra-articular injection of HA-NPs was confirmed in a preclinical rat model.

MATERIALS AND METHODS

Preparation of Core-Shell Nanoparticles

Poly (D, L-Lactic/Glycolic Acid) (PLGA) NPs were produced by a double emulsion and solvent evaporation method [20]. Briefly, bovine serum albumin (25 g/L in water, Sigma, Deisenhofen, Germany) including 5% of BSA coupled with Cyanine-3 (BSA-Cy3, Interchim, Montluçon, France) was transferred in a vial containing PLGA (50% (w:w) lactic acid, 50% (w:w) glycolic acid, Sigma) at 4 g/L dissolved in dichloromethane. The mixture was stirred for one minute with a vortex mixer, and then sonicated (2 min, power 5, 50% active cycle in an ice bath) using a Vibracell model 600 W. This primary emulsion was poured into a second aqueous phase of hyaluronic acid (HA, 5 g/L, BioIberica SA, Barcelona, Spain).

The water in oil in water emulsion was then obtained by sonication (same conditions as those used for the primary emulsion). The organic solvent was evaporated under stirring at 37°C for 2 h, and the slurry of the NPs were resuspended in water and washed twice with water to remove excess HA. The final suspension was then centrifuged, and solid NPs were freeze-dried without cryoprotectant and store at 4°C until further use. The size distribution of nanospheres (mean diameter and standard deviation) was determined by photon correlation spectroscopy using Malvern equipment (Mastersizer MS2000®, Malvern Instrument, Worcestershire, United Kingdom) in 10^{-3} M NaCl (Sigma) at 25°C.

Tissue Procurement and Primary Cell Culture

All experiments with human cells were performed in three independent experiments to prevent patient-dependent variations. Human articular cartilage and synovial membrane were obtained from osteoarthritic patients undergoing total knee replacements. Bone marrow-derived MSCs were obtained from femur samples of patient undergoing total knee or hip replacement surgery for OA. All patients signed informed consent form. This study was approved by our local Research Institution review board (registration number: *UF 9757 - CPRC - Cellules souches et chondrogenèse*). Cells are used for experiments immediately after procurement from human samples, without freezing step (within the two first passages).

Healthy pieces of cartilage were cut off from articular surfaces, minced and rinsed in PBS, stored in a 50-ml conical tube and pre-digested with 2 mg/ml pronase (Sigma) for 2 h at 37°C in NaCl (BBraun, Boulogne Billancourt, France), 0.9%. Then, pronase was removed, cartilage pieces were rinsed with NaCl and digested overnight with 2 mg/ml collagenase B (Roche, Meyland, France) in DMEM culture medium at 37°C under mixing. The enzyme digested supernatant was filtered through 100 µm sterile filters (Millipore, Merck, Darmstadt, Germany) and chondrocytes were collected after centrifugation at 200*g* for 10 min in serum-containing culture medium.

Synoviocytes were obtained after digestion with collagenase B (0,1 U/ml) and dispase (0,8 U/ml, Gibco) at 37°C overnight. The supernatant was filtered through 100 µm sterile filters, and cells were collected after centrifugation at 200*g* for 10 min.

After aspiration in femoral neck, human bone MSCs were cultured in a 75 cm^2 flask with proliferation medium.

Composition of cell culture media is available in supplementary materials.

Internalization Studies

Cells were seeded in 24 well plates at a density of 50000 cells per well, and were exposed to NPs with BSA-Cy3 at 100 µg/ml for 2 to 12 h (one step every 2 h), 24, 48 and 72 h. For fluorescence microscopy observations, cells were seeded on glass coverslips. After exposure to NPs, cells were fixed with 4% paraformaldehyde (Sigma) solution (pH 7.4 for 15 min at room temperature) and washed three times with PBS (Phosphate Buffer Saline, Gibco).

Immunofluorescence was performed after incubation of coverslips with blocking BSA solution (5% in PBS, 20 min at 37°C). Primary antibody against CD44 (Mab7045, R&D Systems) was incubated overnight at 4°C. Coverslips were then washed three times with PBS. FITC conjugated secondary antibody (λem. = 494 nm, sc2010, Santa Cruz Biotechnology, Heidelberg, Germany) was then added for 2 h at room temperature. Slides were mounted with Vectashield Mounting Medium with DAPI (λem. = 358 nm, H-1500, Vector Laboratories, Peterborough, United Kingdom). Cells were examined under an epifluorescence microscope (DMI 3000B, Leica, Nanterre, France) with magnification ×40 (NPs with BSA-Cy3: λem. = 548 nm). Fluorescent observations were realized at each time point to detect particles inside cells. Quantification of encapsulation / internalization efficiency was made only by visual observation of red spots in cells, thanks to the cell membrane labelling. No quantitative data was measured.

To evidence the subcellular localization of internalized NPs, treated cells were washed in PBS and labelled with Lysotracker Green (L7526, Molecular probes, Life technologies). The localization of NPs to lysosomes was demonstrated by co-localization studies using an epifluorescence microscope (DMI 3000B, Leica, >Nanterre, France) with magnification ×40 (BSA-Cy3, λem 570 nm; Lysotracker green, λem 511 nm).

LDH Activity Measurement

Cell viability was evaluated by the measurement of lactate deshydrogenase activity in culture supernatant from 2 to 72 h after particles exposition, with a Cytotoxicity Detection Kit (Roche, France). When damage to the plasma membrane occurs, the cytoplasmic LDH is released in culture supernatant. Briefly, LDH will take part in the reduction of a tetrazolium salt in formazan, thus the increase in the amount of enzyme activity in supernatant directly correlates to the amount of formazan formed during a limited time period. Therefore, the amount of color formed in the assay is proportional to the number of lysed cells. Data were calculated as the percentage of cytotoxicity using the formula: (experimental value − low control/high control − low control) × 100. Where low control corresponds to cells without assay treatment and high control to cells placed in lysis buffer (Triton X-100, 1%, Sigma).

MTT Assay

Mitochondrial activity was evaluated by MTT assay following the same kinetic than for internalization studies. Briefly, after

particles exposure, culture medium is removed and a mixture of 100 µl of MTT (3(4,5-Dimethylthiazol-2-yl)-2,5-diphenyltetrazolium bromide, 5 mg/mL in PBS, Sigma) and 400 µl of culture medium were added per well. Plates were incubated in the dark at 37°C under 5% CO2 for 4 h. The intense purple coloured formazan derivative, formed during active cell metabolism, was eluted and dissolved in a solution containing sodium dodecyl sulfate with dimethylformamide. The absorbance was then measured at 580 nm. Mitochondrial activity results were normalized by DNA quantisation in each well.

Evaluation of Inflammatory Response

Inflammatory response after NPs exposure was assessed based on IL-1ß and TNF-α gene expression (see "*RNA extraction and real-time RT-qPCR analysis*"). In addition, and to confirm RT-qPCR results, prostaglandins E2 (PGE_2) and nitric oxide (NO) levels were measured. Both chondrocytes and synoviocytes have been shown to produce pro-inflammatory mediators [22] that are linked wtih inflammation. They promote the inflammatory reaction, and can contribute to the increase in catabolic processes, leading to cartilage destruction.

Chondrocytes were seeded in 24 well plates at a density of 50000 cells per well, and were exposed to NPs with BSA-Cy3 at 100 µg/ml for 12, 24, 48 and 72 h. Lipopolysaccharide (1 µg/ml, Sigma) was used as positive control to induce inflammatory response by chondrocytes. At each endpoint, supernatants were collected, centrifuged to eliminate cell debris, and frozen at −20°C until analysis.

Nitric Oxide Assay

Nitrite production was determined spectrophotometrically by measuring their accumulation in culture supernatants (number of replicate $n=5$) using the Griess reaction according to the work of Green *et al.* [23]. Briefly, nitrites form a diazonium salt with sulphanilic acid (Sigma) and after addition of N-alpha-naphthyl-ethylenediamine (Sigma) a pink colour develops. Absorbance was measured using a plate reader at 550 nm, and nitrite concentration determined using a standard solution of $NaNO_2$ (Sigma).

Prostaglandin E_2 Measurement

Prostaglandin E_2 synthesis was assessed using a commercial ELISA kit (Parameter™ PGE2, R&D Systems) following manufacturers recommendations. PGE_2, secreted in the culture medium, was determined by a competitive EIA in a 96- well plate using a standard curve (ranging from 39 to 2500 pg/ml) run with each assay. Briefly, PGE_2 in the sample binds to the monoclonal antibody attached in each well. During the second incubation, HRP-labelled PGE_2 binds to the remaining antibody sites. After removing unbound materials, enzyme activity is determined with substrate solution, and absorbance is read at 450 nm. The intensity of the colour is inversely proportional to the concentration of PGE_2 in the sample.

RNA Extraction and Real-Time RT-qPCR Analysis

Total RNA was extracted with the RNeasy kit® (RNeasy Kit, Qiagen, Courtaboeuf, France) following the manufacturer's recommendations. A total of 0.5 µg of RNA from each sample was then reverse-transcribed with High Capacity RNA-to-cDNA Master Mix (Applied Biosystems, Life Technologies) according to the supplier's recommendations.

Real Time Quantitative PCR was performed using TaqMan Fast Universal PCR Master Mix (Applied Biosystems) and commercially available primers (TaqMan gene expression assay, Applied Biosystems) in a StepOnePlus thermocycler (Applied Biosystems). The thermal cycling conditions comprised 2 min at 50°C, 10 min at 95°C, and 40 cycles of 3 s denaturation at 95°C and 30 s annealing at 60°C. Quantification was performed by the comparative Cycle Threshold method to calculate the relative fold change *versus* control, after normalization by our internal standard (RPLP0: ribosomal protein large P0).

Effect of Nanoparticles on Multipotency of MSCs

Composition of specific differentiation media is available in supplementary materials.

Chondrogenic Differentiation

MSCs in monolayer were removed from flasks with trypsin and counted. Pellets were obtained by centrifugation of 1million cells at 300 g for 5 min. Two days later, proliferation medium was removed, and pellets were cultured for 28 days in differentiation medium [24], at normoxia under 5% CO_2 at 37°C in humidified atmosphere. Culture medium is changed every 2 days. Then, pellets are fixed in 4% PFA for histological evaluation, or freeze (−80°C) for RNA extraction.

Osteogenic Differentiation

MSCs were cultured for 15 days in osteogenic medium [25] under standardized conditions.

Adipogenic Differentiation

MSCs in monolayer were induced for adipogenic differentiation during 21 days in dedicated medium [25].

Each experiment was made in four experimental conditions, to assess the respective influence of dedicated culture media and NPs:

- without differentiation medium / without NPs (DM-/NP-)

- without differentiation medium / with NPs (DM-/NP+)
- with differentiation medium / without NPs (DM+/NP-)
- with differentiation medium / with NPs (DM+/NP+)

Assessment of differentiation was performed by quantitative PCR analysis of specific markers and histology: mRNA level of *COL2A1* (a major matrix protein collagen 2), and *COMP* and *ACAN* (two cartilage specific proteins) [26] was used to evaluate chondrogenic differentiation state. Adipogenic differentiation was examined by measurement of mRNA level of *PPARG* (peroxisome proliferator-activated receptor gamma), *LEP* (leptin) and *FABP4* (fatty acid binding protein 4). Osteogenic differentiation was studied by measuring mRNA levels of *ALPL* (alkaline phosphatase), *RUNX2* and *COL10A1* (collagen 10).

Histological Evaluation of MSCs Lineages

Detection of adipocytes

Cells were fixed with 4% paraformaldehyde (PFA) solution (pH 7.4 for 15 min at room temperature) and washed three times with PBS. Vacuoles of lipid droplets were stained by Oil Red O (Sigma): 1% Oil Red O dissolved in 60% isopropanol (Sigma) for 10 min, washed twice with distilled water and counterstained with stabilized Haematoxylin.

Detection of osteoblasts

Cells were fixed with 4% PFA solution (pH 7.4 for 15 min at room temperature) and washed three times with PBS. Calcium deposits were stained by Alizarin Red (2%, pH 4.2, for 5 min, Sigma), and washed with acetone.

Chondrogenic differentiation

Pellets were fixed for 24 h with 4% PFA, and then embedded in paraffin. Sections (5 µm thick) were rehydrated in a graded ethanol series and stained with haematoxylin / eosin / saffron and Alcian blue.

In Vivo Study

Experiments were performed on young male Wistar Han rats (150–175 g, $n=5$ per group) purchased from Charles River Laboratories®, France. The use of animals and experimental protocols, including euthanasia, were conducted following the national animal care guidelines, adhered to the "Principles of Laboratory Animal Care" and were approved by our local ethics committee. NPs were solubilized in 0.9% NaCl (BBraun, Boulogne Billancourt, France) at 1 mg/ml, sonicated for 15 min in an ultrasonic water bath and then sterilized for 10 min with UV light (290 nm). NPs (50 µl at 1 mg/ml in NaCl, as previously optimised [21]) were injected intra-articularly into the right knee, under general anaesthesia, using volatile anaesthetics (Aerrane; Baxter SA, Maurepas, France). Rats treated with *Mycobacterium tuberculosis* cell walls (*MbT*, 500 µg in 50 µl of saline, BD Biosciences) served as positive control to induce inflammation [27]. Negative control was obtained by saline intra-articular injection.

Patella and synovial membrane were collected at necropsy (3 or 7 days after NPs Injection), fixed immediately for 24 h with paraformaldehyde (4%, pH 7.4, Sigma), decalcified in 10% EDTA (Sigma) (patella only), and then embedded in paraffin. Sections (5 µm) were rehydrated and stained with haematoxylin/eosin/saffron, toluidine blue and Sirius red (all from RAL Diagnostics, Martillac, France). These staining allow to observed inflammatory signs, as fibrosis, vascularization, cellular infiltration for synovial membrane, or matrix degradation for cartilage. For fluorescence microscopy observations, sections were rehydrated and mounted with aqueous mounting medium supplemented with DAPI (4′,6-diamidino-2-phenylindole, Vectashield Mounting Medium with DAPI, Vector Laboratories).

Statistical Analysis

Results are expressed as mean ± SD. All analyses and editing of figures were performed using GraphPad Prism 6 (GraphPad Software Inc.). Student's *t*-test was used to compare a batch to its own control and ANOVA with post-hoc Bonferroni's test when required *(e.g.*,groups≥3).

RESULTS

Nanoparticles Uptake by Articular Cells

The size distribution of the particles obtained with a cyanine 3 labelling of the core is d_{50}: 335 nm (median particle size) and $d_{4,3}$: 1533 nm (the mean diameter over volume). A kinetic study of NPs internalization was performed (Fig. 1), in which CD44 immuno-labelling was used to delimit the plasma membrane. At two hours, for both chondrocytes and synoviocytes, we observed particles are around cells, as depicted by plasma membrane labelling. Cells did not internalize particles after 2 h of exposure; this was also confirmed by confocal microscopy observations. Fluorescence imaging suggested that NPs penetrated chondrocytes or synoviocytes after about 8 h of exposure, as shown by the membrane labelling. Although quantification was impracticable, the incorporation of NPs into chondrocytes was constantly more obvious than into synoviocytes as judged from fluorescence microscopy data. In both cell types, the maximum incorporation was reached

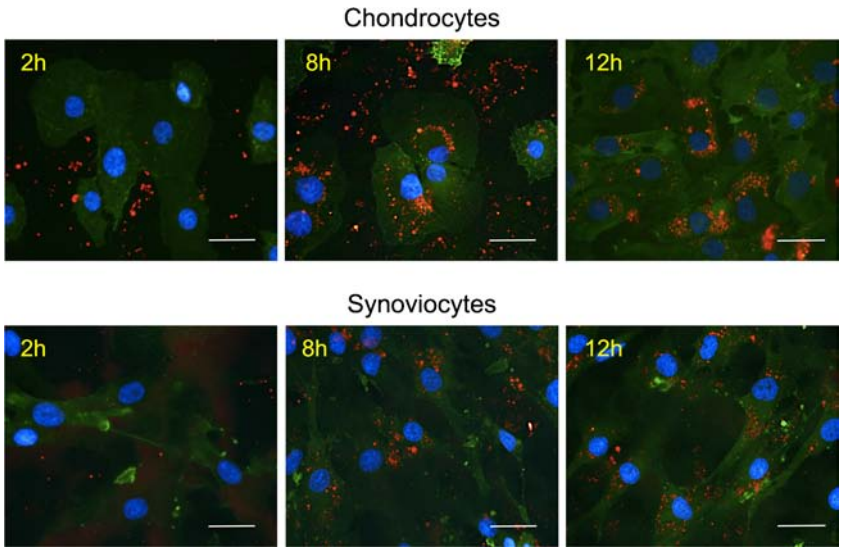

Fig. 1 Internalization of particles. Internalization of NPs in chondrocytes and synoviocytes. In red BSA-Cy3 in nanoparticles, in *blue* nuclear staining with DAPI and in *green*: CD44 immunolabeling. The *size bar* represents 20 μm. Magnification ×40.

at 24 h. On a long time perspective, NPs remained inside cells (in monolayer cultures) for at least 1 to 3 cell passages by trypsinization.

To identify and confirm particles intracellular location, lysosomes were stained with Lysotracker® after NPs exposure (Fig. 2), which revealed that red and green spots can be merged, meaning that NPs are localised inside lysosomes after 24 h of exposure.

In a parallel experiment, the cytotoxicity of these NPs on chondrocytes was monitored by LDH activity measurement and MTT assay following the same kinetic study and up to 72 h (data not shown). After NPs exposure, no effect on cell viability, assessed by LDH activity measurement, was detected. Cell counting at each time point did not detect any difference between NPs and negative control conditions. Yet, a slight decrease of mitochondrial activity between 24 and 72 h of particles exposure was detected by MTT assay ($p<0.001$ *versus* control condition without NPs exposure).

Analysis of Inflammatory Response

For each point of internalization kinetics study (for 2 to 12 h every 2 h and 24/48/72 h), mRNA expression levels of two major pro-inflammatory cytokines *TNF* and *IL1B* were evaluated by RT-qPCR (Fig. 3).

In synoviocytes, NPs exposition led to a significant increase in IL-1ß mRNA expression (Fig. 3(a)), with a 5-fold increase (*versus* control without particles exposure) at 4 h, and a maximum of 7-fold (*versus controls*) at 6 h. Thereafter, expression of *IL-1β* decreased to come back to control levels. Regarding *TNF* (Fig. 3(b)), a maximum of 9-fold increase (*versus* control) was observed after 2 h, but then the expression returned to normal level at 6 h.

In chondrocytes, a similar inflammatory response was observed as in synoviocytes. Exposure to NPs led to an increase of *IL1B* mRNA expression (Fig. 3(c)), peaking at 45-fold *versus* controls at 8 h and then decreasing to basal levels after 24 h (without significant differences *versus* control). For *TNF* (Fig. 3(d)), a 355-fold expression of mRNA *versus* control condition after 4 h of NPs exposure was observed, and a baseline level after 8 h, without significant differences between controls and NPs conditions.

PGE_2 analysis (Fig. 3(e)) shows that LPS stimulation (as archetypal pro-inflammatory stimulus, used here as a positive control) induced a significant induction of PGE_2 production (light grey bar), with a 30-fold expression (*versus* negative control, white bar) for 12 to 48 h, and a 80-fold for 72 h. NPs exposure (dark grey bar)

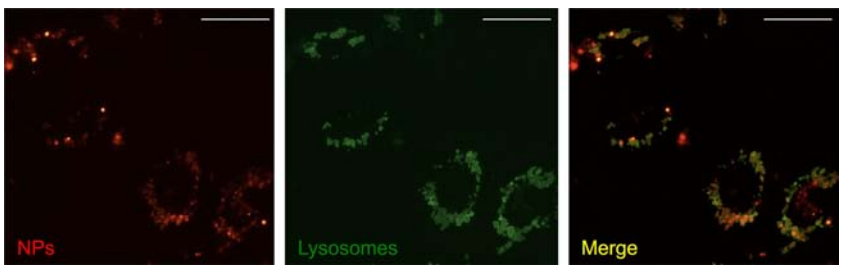

Fig. 2 Subcellular location of particles. Intracellular location of particles in chondrocytes after 12 h of exposure. NPs are *red*, lysosomes are *green* following Lysotracker® labelling. The *size bar* represents 20 μm. Magnification ×40.

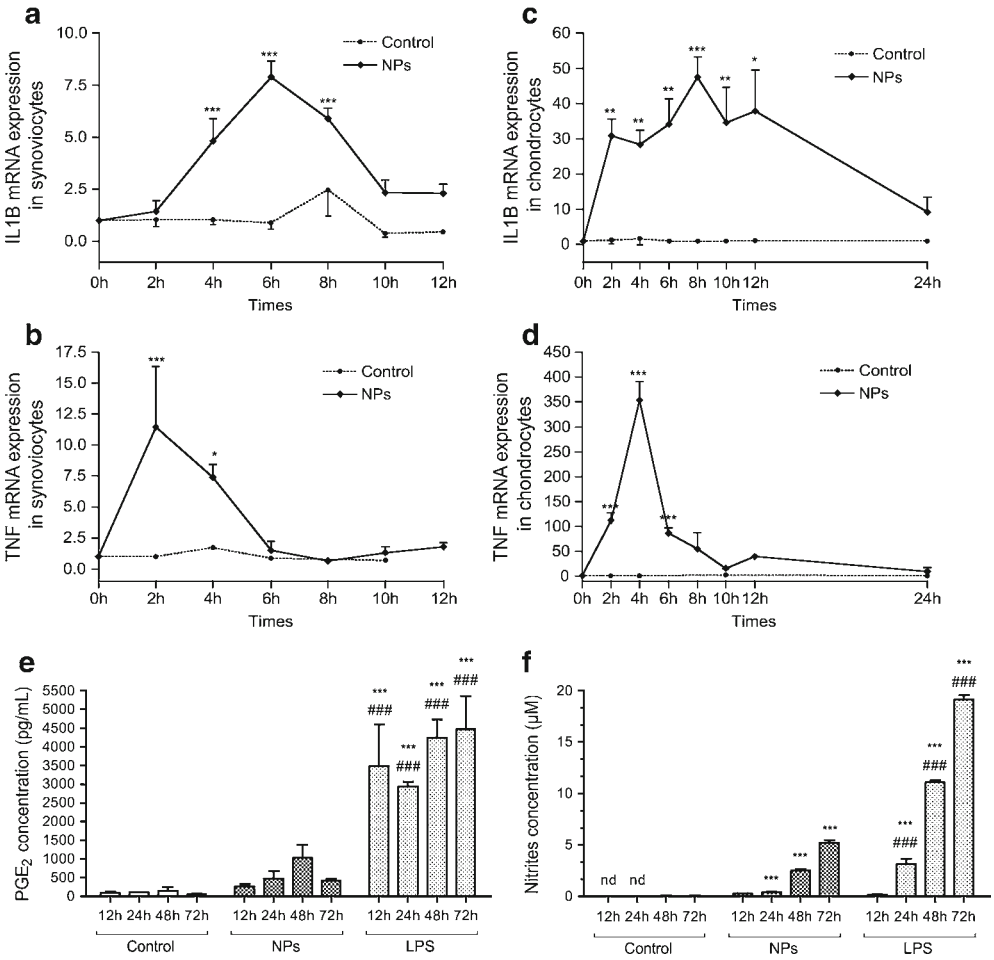

Fig. 3 Inflammatory response following particles exposure. Evaluation of inflammatory markers in chondrocytes and synoviocytes following NPs exposition. **a & b**: Fold expression of IL1B and TNF mRNA in synoviocytes exposed to NPs from 2 to 12 h. **c & d**: Fold expression of IL1B and TNF mRNA in chondrocytes exposed to NPs from 2 to 72 h. Expression's levels at 48 h and 72 h were not detected. PGE2 measurement (**e**) and nitrites assay (**f**) assessed in chondrocytes after NPs exposition. All comparisons of NPs conditions were performed *versus* the control condition at 2 h with a 1-way ANOVA followed by a Bonferonni's test. Data are mean ± SD. *: $p < 0.05$, **: $p < 0.01$, ***: $p < 0.001$, ###: $p < 0.001$ *versus* NPs condition at the same time, nd: not detected.

induced a slight increase of PGE_2 production peaking at 48 h, which, however, remained very moderate, when compared with the positive controls.

Nitrite Oxide. Measurement of nitrite production (Fig. 3(f)) revealed concentrations reaching 2.4 µM at 48 h, and 5.2 µM after 72 h of NPs exposure *versus* 0.06 µM for negative controls (cells cultured in classic medium). This increase remained significantly lower than positive control (LPS), with nitrite concentration of 11.1 µM at 48 h and 19.2 µM at 72 h.

Effects of NPs on Multipotency MSCs

MSCs internalized NPs as seen in synoviocytes and chondrocytes; internalization begun at 8 h and peaked at 24 h (data not shown). This internalization led to similar moderate and transient inflammatory response observed in chondrocytes and synoviocytes (data not shown). After 24 h of NPs exposure, when particles are located inside cells, the capacity of MSCs to differentiate into the three classical pathways (chondrogenic, adipogenic and osteogenic) with purpose-made media [28] was assessed.

Chondrogenesis

Regarding chondrogenic differentiation (in pellets culture system [26]), RT qPCR analysis of specific markers [29] (Fig. 4) revealed that differentiation medium applied on MSCs in pellets, induced an increase of *ACAN* (×450), *COMP* (×40) and *COL2A1* (×10000) mRNAs synthesis (DM+/NP-) *versus* controls without differentiation medium (DM-/NP-). The weak increase of type II collagen observed without differentiation medium and with NPs exposure (DM-/NP+) is not statistically significant. NPs did not affect the capacity of MSCs to differentiate into chondrocytes as, when cultured under differentiation-promoting factors, MSCs with internalized NPs (DM+/NP+) reached very comparable levels of chondrogenic differentiation markers as non-exposed MSCs (DM+/NP-).

These results were confirmed at the extracellular matrix level by histological analysis (Fig. 5(a) & (b)). Culture in differentiation medium without NPs exposition (Fig. 5(a), DM-/

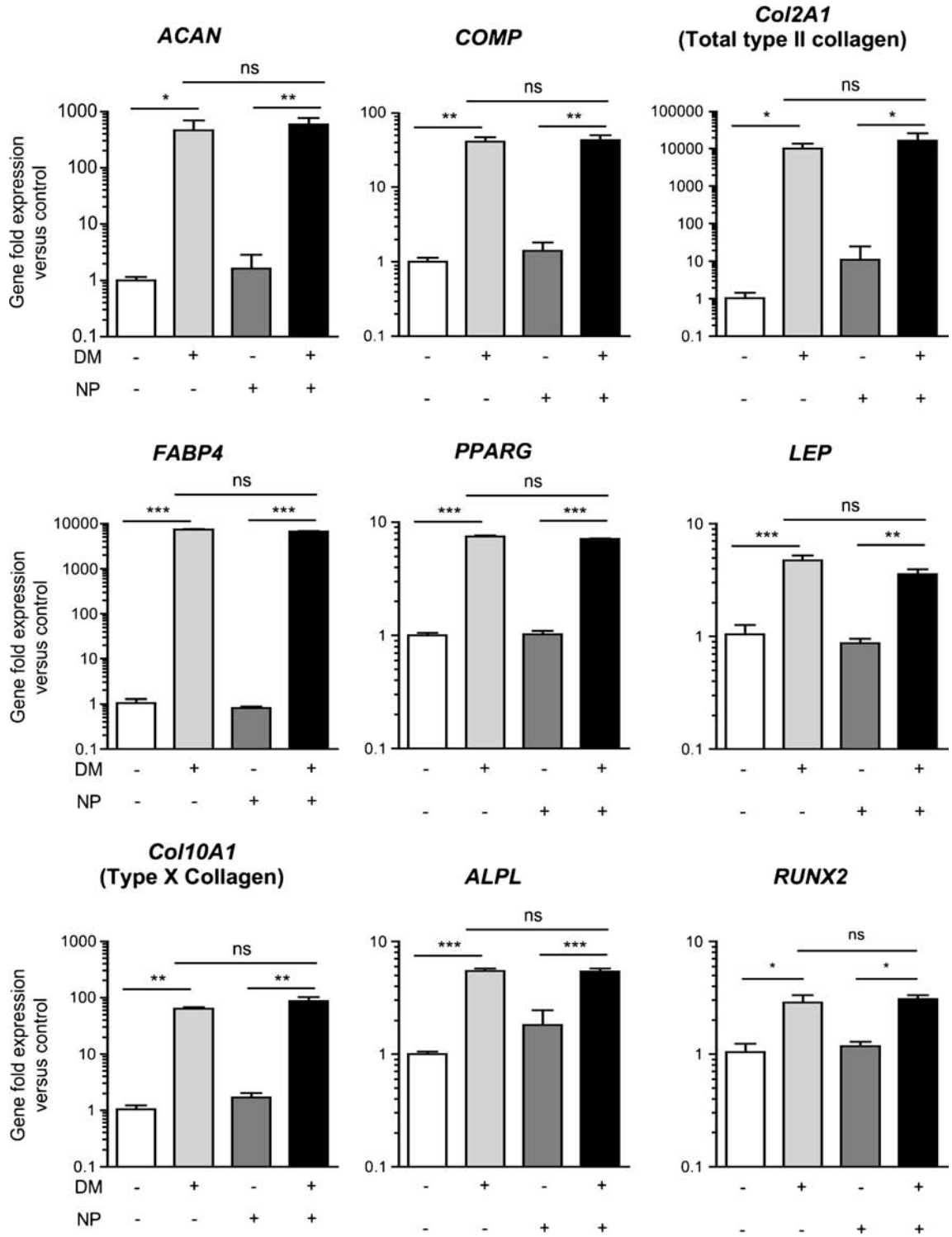

Fig. 4 Mesenchymal stem cell differentiation ability assessed by specific markers measurement. Assessment by quantitative PCR of neutrality of NPs on mesenchymal stem cell differentiation. MSCs are exposed (NP +) or not (NP -) to NPs for 24 h and cultured in control medium (DM -) or in differentiation medium (DM +). **First line**: fold expression of mRNA markers for chondrogenic differentiation. **Second line**: fold expression of mRNA markers of adipogenic differentiation. **Third line**: osteogenic differentiation assessed by marker's mRNA measurement. **DM**: Differentiation medium, **NP**: nanoparticles. Comparisons were performed *versus* each respective control with a 1-way ANOVA followed by a Bonferonni's test. Data are mean ± SD. *: $p < 0.05$, **: $p < 0.01$, ***: $p < 0.001$, ns: not significant.

NP- *versus* DM+/NP-) induced an increase proteoglycan synthesis, as seen in pellets stained with Alcian blue. NPs exposure prior to differentiation medium exposition (5 B) did not affect Alcian Blue intensity (DM+/NP- *versus* DM+/NP+).

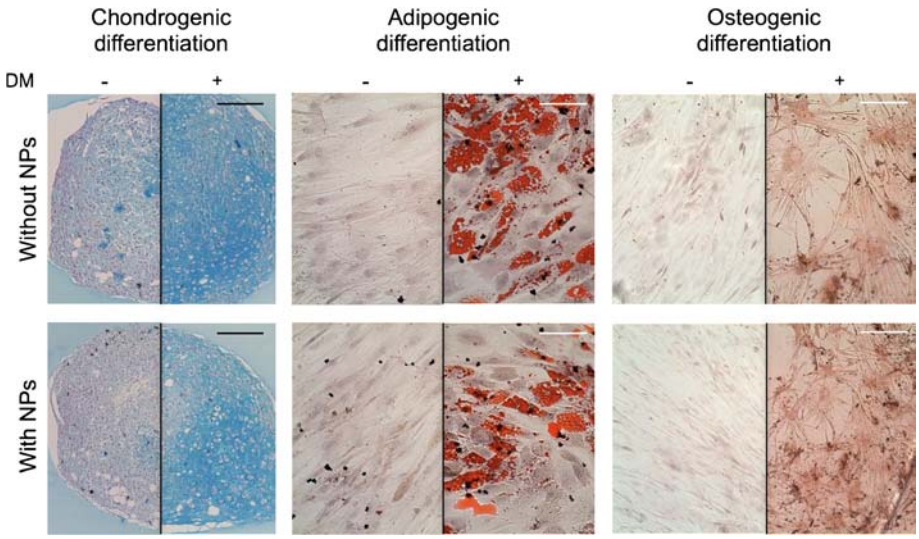

Fig. 5 Histological evaluation of MSCs differentiation after NPs exposition. **a & b**: Alcian Blue staining of proteoglycans in pellets, specific of chondrocytes differentiation. The *black bar scale* represents 200 μm. Magnification ×10. **c & d**: Red Oil O / Haematoxylin staining of lipids vesicles (red spot), specific of adipocytes differentiation. **E & F**: Alizarin Red staining of calcium deposits, a marker of osteoblastic differentiation. **C**–**F**: The *white bar scale* represents 100 μm. Magnification ×20. **DM**: Differentiation medium.

Adipogenesis

Without NPs exposition, differentiation medium (DM+/NP- *versus* DM-/NP-) led to a significant increase of mRNA synthesis: (Fig. 4) 7200-fold for *FABP4*, 7.4-fold for *PPARG* and 4.7 for *LEP*. NPs exposition did not affect adipogenic marker expression. Red Oil O staining of lipid vesicles confirmed adipogenic differentiation at the cellular level, staining intensity being not influenced by NPs exposition (DM+/NP- *versus* DM+/NP+, Fig. 5(c) & (d)).

Osteogenesis

As expected, differentiation medium provoked an increase of dedicated mRNA (Fig. 4): 63-, 5.4- and 2.8-fold for *COL10A1*, *ALPL* and *RUNX2* respectively (DM+/NP- *versus* DM-/NP-). NPs exposition before differentiation induction did not significantly modify markers expression (DM+/NP- *versus* DM+/NP+). Alizarin Red staining of calcium deposits (Fig. 5(e) & (f)) confirmed these results, coloration intensity being similar after NPs exposition (DM+/NP- *versus* DM+/NP+).

Effects of Intra-Articular Injection in Rats Knees

First, following intra-articular injection of particles, no sign of swelling, oedema or lameness was detected visually on rats. Their mobility was not clinically affected by injections.

Taking advantage of the red fluorescence specifically developed for these particles, we observed seven days post injection that NPs localized mainly to the inner layer of the synovial membrane (Fig. 6(a)–(c)). We found only some spots on cartilage surface and in outlying fibrocartilage.

Histological analyses of synovial membranes stained by Haematoxylin Eosin Saffron (Fig. 6(d)) were performed at 3 and 7 days post-injection to investigate a possible inflammatory reaction. Captions revealed a weak hyperplasia of inner layer of synovial membrane for rats injected intra-articularly with saline injection (50 µl) at days 3 and 7. We did not observe any evidence of increased vascularization, fibrosis, or immune cell infiltration upon NPs exposure, however, both inflammation criteria was strongly induced by the injection of *M. tuberculosis* cell wall, 10 mg/ml positive control of acute inflammatory reaction.

With reference to patellae, HES staining of cartilage slices (Fig. 6(e)) on day 7 did not reveal any changes in cell repartition whatever the cartilage zone, cartilage thickness and surface (neither fibrillations nor fissures), and subchondral bone remodelling in both saline (50 µl) and NPs (50 µl at 1 mg/ml in saline) groups, in contrast to the *M. tuberculosis* positive control. Sirius red staining intensity of collagen or toluidine blue staining intensity of proteoglycans in cartilage matrix was similar for both NPs and saline groups, contrasting with marked depletion in positive control of inflammation.

DISCUSSION

Tracking of nano objects is one of the challenges in nanomedicine. In numerous studies, it has been necessary to tag the incorporated compound [6] (which can affect the native properties of the compound), or to encapsulate a fluorescent molecule instead of an active molecule [9] in order to detect NPs. To this end, different amounts of BSA-Cy3 were tested in a previous work to determine a quantity without deleterious effects on NPs structure/properties, but sufficient to enable a fluorescent tracking (unpublished personal data).

Improvements made by our team in the synthesis process, in collaboration with chemists, allowed us to label the NPs structure, thus enabling its tracking, whatever the encapsulated compound and without affecting NPs physical properties.

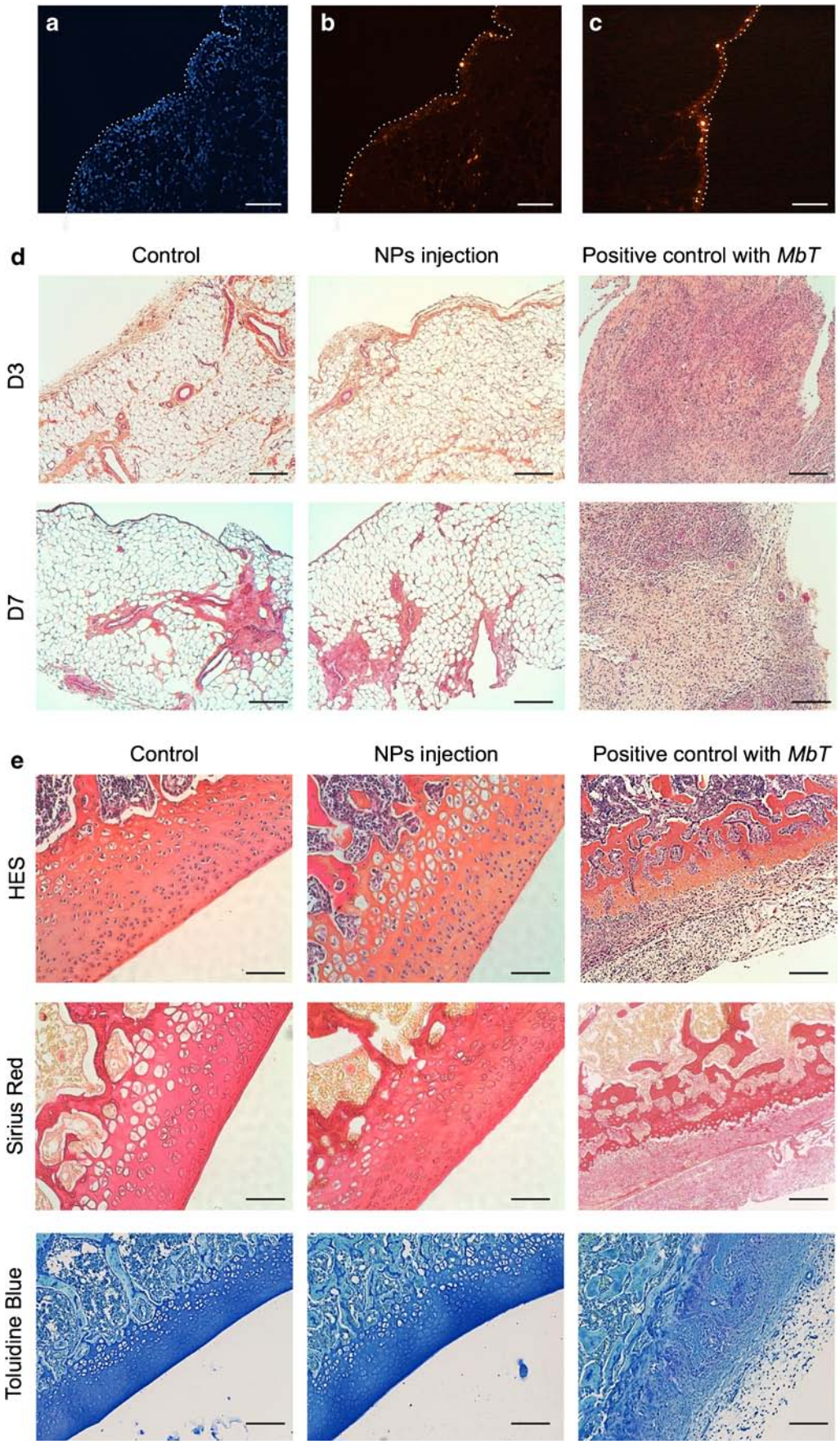
a
b
c
d
Control
NPs injection
Positive control with MbT
D3
D7
e
Control
NPs injection
Positive control with MbT
HES
Sirius Red
Toluidine Blue

◀ **Fig. 6** Histological exams of rat knees following particles exposition. Fluorescent microscopy picture of synovial membrane (**a**, **b**) and patellae (**c**) of rats. In *red* (λem: 548 nm): nanoparticles, in *blue* (λem: 358 nm): nuclear staining with DAPI. The *white dotted line* (**a**, **b & c**) shows the limit of the tissue and the articular cavity. Magnification ×40, the *white bar scale* represents 100 μm. **d**: Histological sections of synovial membrane (HES staining) of rats 3 or 7 days after NPs injections (1 mg/ml). **e**: HES staining of cells repartition, collagen staining with sirius red and toluidine blue staining of proteoglycans in patellae of rats 7 days after NPs injections (1 mg/ml). Injection of *Mycobacterium tuberculosis* cell wall (10 mg/ml) served as positive control of inflammation. $n = 5$ for each group. Magnification ×10, the *black size bar* represents 200 μm.

In this work we have studied the effect of a BSA-Cy3 labelling of the core of PLGA particles (using core-shell particles previously described [21]) for articular cell targeting. We have focused on safety studies after particle internalization in two major cell types found in knee joint, *i.e.,* chondrocytes and synoviocytes. In order to appreciate different aspects of particles' neutrality, we have also focused on a pluripotent cell type, MSCs, and assessed the functionality after NPs loading.

We have confirmed that NPs are internalized by synoviocytes and chondrocytes between eight and 10 h, and NPs remained inside cells at least for 96 h *in vitro* (unpublished internal data). Previous experiments have shown that an antibody directed against CD44 competes with HA-NPs for binding to receptors expressed on cell membranes [20]. As demonstrated in cancer cells [4] and in previous work for chondrocytes targeting [17], HA / CD44 recognition plays an active role in the internalization process in articular cells. In previous experiment, we have confirmed that internalization of cyanine-3 labelled, HA covered NPs was almost totally suppressed after CD44 blockade with a specific antibody. On the other hand, using specific labelling of Golgi apparatus, endoplasmic reticulum and lysosomes we confirmed the lysosomal location of NPs after 24 h of exposure as previously mentioned by *Danhier et al.* [4]. In lysosomes, degradation of NPs will be initiated, but earlier studies reported [30] a rapid exit from the lysosomal compartment to the cytoplasm where NPs can release the encapsulated compound. This interesting property allows to deliver the encapsulated compound directly inside the cells, close to the nucleus (*e.g.,* for the transport of nucleic acid). We have also demonstrated that NPs stay inside cells for long time (up to three passages).

As intra-articular administration can induce acute phlogistic / inflammatory severe reactions, we have verified that exposure to particles did not lead to deleterious reactions. Besides, NPs exposure induces only slight and reversible inflammatory response, as revealed by real-time RT-qPCR analysis, and subsequent confirmation with PGE_2 and NO measurements. This response remains transient and is significantly lower than that the one induced by LPS.

On gene expression analyses, the peak of inflammatory reaction markers was observed between two and six hours, whereas particles are not detected inside cells before eight hours of exposure. We can hypothesize that this weak and reversible inflammatory response could be induced by the contact of NPs with cells, and not as a specific response to NPs internalization. Thus, such internalization seems to be well tolerated by articular cells, without elicitation of a massive inflammatory response. The non-immunogenic nature of the nano-object confirms the biocompatibility of all components of the newly labelled particle's structure.

Since these particles are designed to be injected intra-articularly and may be internalized by surrounding resident cells, we wanted to ensure that the internalization process did not compromise cell functionality/viability. As outlined by *Nicolete et al.* [31], NPs could exert an inflammatory response on macrophages or enhance other inflammatory stimulus after uptake process. Experiments on synovial fibroblasts have shown that, when cells are stimulated by LPS or IL-1ß, NPs exposure, prior to or after stimulation, does not interfere with ancillary inflammatory response. Similarly, the internalization of NPs did not affect extracellular matrix synthesis by chondrocytes, suggesting a lack of deleterious influence of NPs on this parameter.

We hypothesize that in pathological (degenerative and/or inflammatory) conditions, when matrix synthesis is altered, the behaviour of NPs will be quite similar. NPs will disturb neither cell homeostasis, nor matrix synthesis ability of resident cells. On the other hand, NPs in cytoplasm will neither disrupt existing inflammatory reaction, nor aggravate it. These facts allow the use of this kind of drug vectorization for rheumatic conditions.

In pathological situations such as osteoarthritis, local MSCs could be recruited to lesions to initiate wound healing [32] from different locations (bone marrow, synovial membrane, …). Recent studies suggest the efficacy of providing autologous BM-MSCs by intra-articular injection to treat patients with cartilage diseases [33]. MSCs are capable of differentiation into chondrocyte-like cells in the presence of a supplemented medium. Analysis of the chondrogenic potential of MSCs revealed that they have a multipotential capability and their chondrogenic capacity could be useful for future cell therapy in articular disease. Chondrogenic loaded NPs may be an interesting alternative to rAAV-mediated (recombinant adeno-associated virus) gene transfer into MSCs for chondrogenic preconditioning, *e.g.,* by integrating dedicated miRNA, antagomirs or siRNA [34].

Since these cells could internalize and retain such NPs, we have assessed whether MSCs differentiation ability (to osteogenic, adipogenic and chondrogenic pathways) is affected by NPs internalization. We have demonstrated that once MSCs have internalized particles, they can still be conducted to their major differentiation pathways without altering their functionality. Likewise, based on the biocompatibility of particles and their persistence inside cells, we could consider using these fluorescent nano-objects to tag MSCs (before or without differentiation induction) in order to track them once injected

either in pathological sites [2] or after seeding in scaffolds. MSCs are also used in tissue engineering [35] to build cartilage tissue. Bringing growth factors (TGF-ß, FGF) or specific genes (Sox9) with particles could facilitate chondrogenic differentiation and matrix synthesis.

Taking advantage of the cyanine-3 labelling, we observed that NPs are preferentially localized to the synovial membrane, which is known to have a filtering role in diarthrodial joints, as previously noticed by *Butoescu et al.* [36]. The weak internalization in cartilage and chondrocytes could be explained by the density of the chondral extracellular matrix, which could partially restrict NPs penetration due to their size [37]. In this regard, degenerative OA lesions, such as fibrillation, could facilitate the accessibility of NPs to damaged chondrocytes. Histological observations of healthy rat knee joints after intra articular injection are consistent with our *in vitro* data. Through analyses of joint tissues following saline (negative control), *M. Tuberculosis* cell wall (positive control), or NPs injections, we found that NPs induced a very weak signs of inflammatory reaction at days 3 and 7. Besides, no structural damages were depicted histologically. Thus, we hypothesize this drug delivery system could bring an anti-inflammatory compound to synovial membrane, which have a major role in inflammatory reaction [38]. This could also prevent the use of viral vectors for delivery of therapeutic genes, as r-AAV systems [39].

CONCLUSIONS

In conclusion, all these data suggest that intra-articular PLGA nano-devices target primarily synovial cells, are not deleterious, and that their intra-cellular degradation does not provoke obvious harmful effects. This PLGA based drug delivery system could be used safely to deliver an active molecule to the joint; when we will encapsulate active compound, all biological effects observed will be due to the molecule and not to a collateral effect of the particle structure. Moreover, these data could be confirmed in experimental degenerative (OA) and inflammatory conditions, to ensure the neutrality of the device in pathological situation, and complement the validation of the drug delivery system for *in situ* chondrocyte rejuvenation during OA.

ACKNOWLEDGMENTS AND DISCLOSURES

We thank David Moulin and Jean-Baptiste Vincourt for their critical reading of the manuscript, Michel Thiery for his good care of the animals and Naranayan Venkatesan for English editing.

The authors declare they have no conflict of interest.

Funding This work was supported by grants from Agence Nationale de la Recherche – programme ANR Blanc 2007: Nanostructured polymers as drug carriers for cartilage repair and engineering (PARTICART, ANR-07-1_1831-56) and grants from the Région Lorraine Communauté Urbaine du Grand Nancy, and Conseil Général de Meurthe et Moselle.

The funding agency had no role in study design, data collection and analysis, decision to publish, or preparation of the manuscript.

Ethical Approval All procedures performed in studies involving animals were in accordance with the ethical standards of the institution or practice at which the studies were conducted.

REFERENCES

1. Mundargi RC, Babu VR, Rangaswamy V, Patel P, Aminabhavi TM. Nano/micro technologies for delivering macromolecular therapeutics using poly(D, L-lactide-co-glycolide) and its derivatives. J Control Release. 2008;125:193–209.
2. Jorgensen C. Mesenchymal stem cells: uses in osteoarthritis. J Bone Spine Rev Rhum. 2013;80:565–7.
3. Sah H, Thoma LA, Desu HR, Sah E, Wood GC. Concepts and practices used to develop functional PLGA-based nanoparticulate systems. Int J Nanomedicine. 2013;8:747–65.
4. Danhier F, Ansorena E, Silva JM, Coco R, Le Breton A, Préat V. PLGA-based nanoparticles: an overview of biomedical applications. J Control Release. 2012;161:505–22.
5. Benfer M, Kissel T. Cellular uptake mechanism and knockdown activity of siRNA-loaded biodegradable DEAPA-PVA-g-PLGA nanoparticles. Eur J Pharm Biopharm. 2012;80:247–56.
6. Zhang X, Sun M, Zheng A, Cao D, Bi Y, Sun J. Preparation and characterization of insulin-loaded bioadhesive PLGA nanoparticles for oral administration. Eur J Pharm Sci. 2012;45:632–8.
7. Reix N, Parat A, Seyfritz E, Van der Werf R, Epure V, Ebel N, *et al.* In vitro uptake evaluation in Caco-2 cells and in vivo results in diabetic rats of insulin-loaded PLGA nanoparticles. Int J Pharm. 2012;437:213–20.
8. Lotz S, Goderie S, Tokas N, Hirsch SE, Ahmad F, Corneo B, *et al.* Sustained levels of FGF2 maintain undifferentiated stem cell cultures with Biweekly feeding. Pereira LV, editor. PLoS ONE. 2013;8, e56289.
9. Pamujula S, Hazari S, Bolden G, Graves RA, Chinta DD, Dash S. Cellular delivery of PEGylated PLGA nanoparticles. J Pharm Pharmacol. 2012;64:61–7.
10. Ding H, Yong K-T, Roy I, Hu R, Wu F, Zhao L, *et al.* Bioconjugated PLGA-4-arm-PEG branched polymeric nanoparticles as novel tumor targeting carriers. Nanotechnology. 2011;22:165101.
11. Obermajer N, Kocbek P, Repnik U, Kuznik A, Cegnar M, Kristl J, *et al.* Immunonanoparticles–an effective tool to impair harmful proteolysis in invasive breast tumor cells. FEBS J. 2007;274:4416–27.
12. Arpicco S, De Rosa G, Fattal E. Lipid-based nanovectors for targeting of CD44-overexpressing tumor cells. J Drug Deliv. 2013;2013:860780.
13. Platt VM, Szoka Jr FC. Anticancer therapeutics: targeting macromolecules and nanocarriers to hyaluronan or CD44, a hyaluronan receptor. Mol Pharm. 2008;5:474–86.
14. Campo GM, Avenoso A, Campo S, D'Ascola A, Nastasi G, Calatroni A. Small hyaluronan oligosaccharides induce inflammation by engaging both toll-like-4 and CD44 receptors in human chondrocytes. Biochem Pharmacol. 2010;80:480–90.

15. Wu S-C, Chen C-H, Chang J-K, Fu Y-C, Wang C-K, Eswaramoorthy R, *et al.* Hyaluronan initiates chondrogenesis mainly *via* CD44 in human adipose-derived stem cells. J Appl Physiol. 2013;114:1610–8.
16. Knudson W, Chow G, Knudson CB. CD44-mediated uptake and degradation of hyaluronan. Matrix Biol J Int Soc Matrix Biol. 2002;21:15–23.
17. Chen Z, Chen J, Wu L, Li W, Chen J, Cheng H, *et al.* Hyaluronic acid-coated bovine serum albumin nanoparticles loaded with brucine as selective nanovectors for intra-articular injection. Int J Nanomedicine. 2013;8:3843–53.
18. Nam JL, Ramiro S, Gaujoux-Viala C, Takase K, Leon-Garcia M, Emery P, *et al.* Efficacy of biological disease-modifying antirheumatic drugs: a systematic literature review informing the 2013 update of the EULAR recommendations for the management of rheumatoid arthritis. Ann Rheum Dis. 2014;73:516–28.
19. Holland C, Jaeger L, Smentkowski U, Weber B, Otto C. Septic and aseptic complications of corticosteroid injections: an assessment of 278 cases reviewed by expert commissions and mediation boards from 2005 to 2009. Dtsch Ärztebl Int. 2012;109:425–30.
20. Laroui H, Grossin L, Léonard M, Stoltz J-F, Gillet P, Netter P, *et al.* Hyaluronate-covered nanoparticles for the therapeutic targeting of cartilage. Biomacromolecules. 2007;8:3879–85.
21. Zille H, Paquet J, Henrionnet C, Scala-Bertola J, Leonard M, Six JL, *et al.* Evaluation of intra-articular delivery of hyaluronic acid functionalized biopolymeric nanoparticles in healthy rat knees. Biomed Mater Eng. 2010;20:235–42.
22. Kapoor M, Martel-Pelletier J, Lajeunesse D, Pelletier J-P, Fahmi H. Role of proinflammatory cytokines in the pathophysiology of osteoarthritis. Nat Rev Rheumatol. 2011;7:33–42.
23. Green LC, Wagner DA, Glogowski J, Skipper PL, Wishnok JS, Tannenbaum SR. Analysis of nitrate, nitrite, and [15 N]nitrate in biological fluids. Anal Biochem. 1982;126:131–8.
24. Roeder E, Henrionnet C, Goebel JC, Gambier N, Beuf O, Grenier D, *et al.* Dose–response of superparamagnetic iron oxide labeling on mesenchymal stem cells chondrogenic differentiation: a multi-scale in vitro study. PLoS One. 2014;9, e98451.
25. Zhang J, Pan T, Im H-J, Fu FH, Wang JHC. Differential properties of human ACL and MCL stem cells may be responsible for their differential healing capacity. BMC Med. 2011;9:68.
26. Demoor M, Ollitrault D, Gomez-Leduc T, Bouyoucef M, Hervieu M, Fabre H, *et al.* Cartilage tissue engineering: molecular control of chondrocyte differentiation for proper cartilage matrix reconstruction. Biochim Biophys Acta. 1840;2014:2414–40.
27. Paquet J, Henrionnet C, Pinzano A, Vincourt J-B, Gillet P, Netter P, *et al.* Alternative for anti-TNF antibodies for arthritis treatment. Mol Ther. 2011;19:1887–95.
28. Méndez-Ferrer S, Michurina TV, Ferraro F, Mazloom AR, MacArthur BD, Lira SA, *et al.* Mesenchymal and haematopoietic stem cells form a unique bone marrow niche. Nature. 2010;466:829–34.
29. Ronzière MC, Perrier E, Mallein-Gerin F, Freyria A-M. Chondrogenic potential of bone marrow- and adipose tissue-derived adult human mesenchymal stem cells. Biomed Mater Eng. 2010;20:145–58.
30. Panyam J, Zhou W-Z, Prabha S, Sahoo SK, Labhasetwar V. Rapid endo-lysosomal escape of poly(DL-lactide-co-glycolide) nanoparticles: implications for drug and gene delivery. FASEB J. 2002;16:1217–26.
31. Nicolete R, dos Santos DF, Faccioli LH. The uptake of PLGA micro or nanoparticles by macrophages provokes distinct in vitro inflammatory response. Int Immunopharmacol. 2011;11:1557–63.
32. Sekiya I, Ojima M, Suzuki S, Yamaga M, Horie M, Koga H, *et al.* Human mesenchymal stem cells in synovial fluid increase in the knee with degenerated cartilage and osteoarthritis. J Orthop Res. 2012;30:943–9.
33. Toupet K, Maumus M, Luz-Crawford P, Lombardo E, Lopez-Belmonte J, van Lent P, *et al.* Survival and biodistribution of xenogenic adipose mesenchymal stem cells is not affected by the degree of inflammation in arthritis. PLoS One. 2015;10, e0114962.
34. Rey-Rico A, Frisch J, Venkatesan JK, Schmitt G, Madry H, Cucchiarini M. Determination of effective rAAV-mediated gene transfer conditions to support chondrogenic differentiation processes in human primary bone marrow aspirates. Gene Ther. 2015;22:50–7.
35. Vinatier C, Mrugala D, Jorgensen C, Guicheux J, Noël D. Cartilage engineering: a crucial combination of cells, biomaterials and biofactors. Trends Biotechnol. 2009;27:307–14.
36. Butoescu N, Seemayer CA, Foti M, Jordan O, Doelker E. Dexamethasone-containing PLGA superparamagnetic microparticles as carriers for the local treatment of arthritis. Biomaterials. 2009;30:1772–80.
37. Rothenfluh DA, Bermudez H, O'Neil CP, Hubbell JA. Biofunctional polymer nanoparticles for intra-articular targeting and retention in cartilage. Nat Mater. 2008;7:248–54.
38. Choy EHS, Panayi GS. Cytokine pathways and joint inflammation in rheumatoid arthritis. N Engl J Med. 2001;344:907–16.
39. Evans CH, Ghivizzani SC, Robbins PD. Arthritis gene therapy and its tortuous path into the clinic. Transl Res J Lab Clin Med. 2013;161:205–16.